Kinetics of Surface Crystallization in Thin Films of Poly(ethylene terephthalate)

Paul C. Jukes,[†] Arindam Das,[‡] Martin Durell,[‡] Dean Trolley,[‡] Anthony M. Higgins,[†,⊥] Mark Geoghegan,[†] J. Emyr Macdonald,[*,‡] Richard A. L. Jones,[†] Simon Brown,[§] and Paul Thompson[§]

Department of Physics and Astronomy, University of Sheffield, Hounsfield Road, Sheffield S3 7RH, UK; Department of Physics and Astronomy, Cardiff University, PO Box 913, Cardiff CF2 3YB, UK; and XMaS Beamline, ESRF, BP 220, F-38043 Grenoble Cedex, France

Received May 13, 2004; Revised Manuscript Received December 15, 2004

ABSTRACT: In-situ grazing incidence X-ray diffraction has been used to investigate the kinetics of crystallization at the surface of thin films of poly(ethylene terephthalate) (PET). By varying the angle of incidence of the X-ray beam around the critical angle of the film, the penetration depth can be tuned to allow a direct comparison of molecular ordering in the surface and bulk of the film. The results show that ordering occurs significantly faster at the surface in the temperature range 90−100 °C (close to the bulk glass transition temperature of 75 °C). The (0 $\bar{1}$ 1) and (0 1 0) peaks narrow more rapidly and achieve a lower width, indicating that the crystallization progresses more rapidly in these crystallographic directions. This enhanced ordering is attributed to a combination of surface energy effects, which promote localized packing, and to an enhanced segmental mobility near the free surface.

Introduction

A fundamental understanding of the influence of free surfaces and buried interfaces on the properties of thin polymer films is important in many applications. For example, in the growing field of polymer-based electronic devices, the structure of interfaces is a crucial factor in determining key properties such as charge transport, recombination, and dissociation,[1−3] and it is only recently that the first experiments to understand the structural issues have been undertaken.[2,3] Near interfacial boundaries, surface, and interface effects may lead to physical properties that significantly differ from those in the bulk, such as the chain conformation,[4] chain dynamics,[5] and the demixing of multicomponent blends.[6,7] A combination of surface- and finite-size effects may also influence the character and location of the crystallization[8,9] and glass transitions.[10,11]

Crystallization at the surface of a semicrystalline polymer thin film may be affected by both changes in chain conformation near the surface and by differences in chain dynamics between surface and bulk. Polymer chains within a radius of gyration of the surface are constrained not to cross the interface between polymer and air, since polymer−air interactions are less energetically favorable than those between polymer segments. Simulation shows that surface energy effects promote a tendency for chain segments to lie flat and parallel to the surface in localized alignment with neighboring chains.[12] Such localized alignment could act as a precursor to crystallization. Alternatively, a spinodal-type mechanism, characterized by long-range orientational fluctuations detected before the appearance of crystalline Bragg peaks, is proposed as an induction phase for polymer crystallization.[13]

Regarding the chain dynamics, observations of reduced glass transition temperatures in thin polymer films can be explained in terms of a layered model with a liquidlike layer of enhanced mobility near the surface.[11,14] In a semicrystalline polymer such as poly(ethylene terephthalate) (PET), an enhanced mobility at the surface in tandem with localized alignment may lead to a lower crystallization temperature and increased kinetics at the free surface. In a previous publication,[8] we reported crystalline ordering of the near-surface region of PET at temperatures where the bulk of the film remained amorphous. PET is an archetypal semicrystalline polymer consisting of rigid aromatic subunits connected by flexible ethyl groups, with a glass transition temperature (T_g) of 75 °C. The structure of PET is shown in Figure 1. Local ordering near the surface of PET was previously investigated using combined XPS and FTIR studies to probe conformational changes associated with crystallization.[15] These experiments showed that the ordering process occurred significantly faster at the surface than in the bulk of a thin film, although it should be stressed that the techniques they employed are only sensitive to local, intrachain effects rather than the longer range ordering measured in our experiments. In another work, spectroscopic ellipsometry was used to detect a reduced T_g of 56 °C for the near-surface region of PET,[16] providing further evidence for a region of enhanced chain mobility near the polymer−air interface.

Long-range surface and bulk ordering in the films was characterized using grazing incidence X-ray diffraction (GIXRD). This technique was first applied to thin polymer films by Factor et al.[17,18] and has more recently been used to investigate molecular ordering in thin films of the conjugated polymers polyfluorene[19,20] and poly(3-hexylthiophene).[21] The power of the technique lies in the fact that the X-ray penetration depth can be tuned

[†] University of Sheffield.
[‡] Cardiff University.
[§] XMaS Beamline.
[⊥] Present address: Multidisciplinary Nanotechnology Centre, School of Engineering, University of Wales Swansea, Singleton Park, Swansea SA2 8PP.
* Corresponding author. E-mail macdonald@cardiff.ac.uk.

10.1021/ma0490606 CCC: $30.25 © 2005 American Chemical Society
Published on Web 02/17/2005

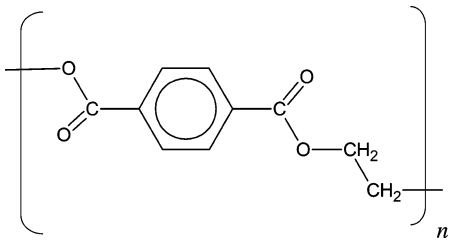

Figure 1. Chemical structure of PET.

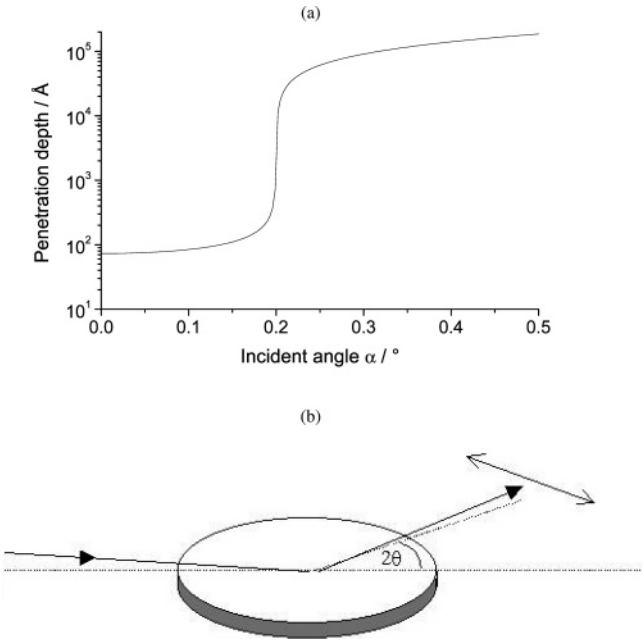

Figure 2. (a) X-ray penetration depth as a function of incident angle for PET with a critical wavevector of 0.0143 $Å^{-1}$. (b) Schematic illustrating the GISPS geometry used for measurements.

by varying the incidence angle of the incoming beam, as shown in Figure 2a. By employing an angle of incidence α less than the critical angle α_c (typically of the order of 0.20°), the penetration of the X-ray beam can be limited to approximately 50 Å, allowing surface-sensitive measurement. For larger values of α above the critical angle, the beam penetrates through the bulk of the film into the substrate, and the bulk scattering is measured. The other principal advantage of the technique is that the structure both in the plane and out of the plane of the sample surface can be probed by employing one of two different scattering geometries. The principal geometry used in this work is the grazing incidence surface-plane scattering (GISPS) geometry, illustrated in Figure 2b. In this geometry, the exit angle is kept equal to the (small) incident angle of the X-ray beam, and the detector is swept horizontally. The scattering vector Q is then primarily defined by the azimuthal displacement of the exit beam, giving information about correlations parallel to the sample surface and in-plane structure. A second geometry, referred to but not employed here, is grazing incidence asymmetric Bragg scattering (GIABS) in which the diffracted beam and the scattering vector Q are in the plane defined by the incident beam and the surface normal. This gives information primarily about correlations normal to the sample surface. An earlier ex-situ annealing study showed that the GIABS geometry is far less sensitive to the earlier stages of crystallization:[8] GIABS scans were not undertaken here due to beamtime constraints. To obtain the results presented here, two angles of incidence were used in the in-plane, GISPS geometry: α = 0.18° for surface-sensitive scans, and α = 0.60 °C for bulk measurements for time series of diffraction scans during in-situ anneals over a range of temperatures.

In this paper we present the results of grazing incidence X-ray diffraction experiments with in-situ annealing of the surface and bulk of thin PET films to quantify the kinetics of surface ordering and to investigate the influence of this on bulk crystallization. We show that ordering is more rapid at the surface than in the bulk of the film and present quantitative results characterizing the kinetics of surface and bulk crystallization.

Experimental Section

The polymer used in this work was additive-free PET, M_n = 25 000 Da, supplied by ICI plc. Thin film samples were prepared by spin-casting onto silicon wafers from a 4% (w/w) solution in *o*-chlorophenol. The as-spun films were baked in a vacuum oven at 40 °C for 24 h to remove residual solvent, resulting in a uniform film of thickness ∼1100 Å. The surfaces of the as-spun films had typical roughnesses of 0.33 nm as measured by AFM. Measurements were taken on the XMaS beamline at the European Sychrotron Radiation Facility (ESRF), Grenoble, France. The X-ray wavelength of 1.6 Å was selected by successive reflections from two Si(111) monochromator crystals in the nondispersive setting following reflection from a toroidal focusing mirror. The beam size of 1.0 × 0.5 mm was defined by four-jaw slits before the sample. Two sets of four-jaw slits on the detector arm were used to define the resolution and the surface area on the sample from which scattered radiation was collected by a Ge solid-state detector. The incident angle was determined experimentally with a precision of ±0.005° by (i) α-scans through the polymer diffuse scattering which give a maximum at the critical angle (ii) transverse scans through the specularly reflected beam. In practice, the first of these gives a more precise value of the incident beam angle α and can be performed with the diffractometer settings used for the main scans. The scattered radiation from a thin beryllium film was used as a monitor for the incident beam flux. The samples were annealed on a hot stage situated inside a custom-built furnace featuring an evacuated, hemispherical beryllium dome allowing 2π solid angle access to the X-ray beam. Use of the vacuum furnace, in which the pressure was about 10^{-5} mbar, achieved a significant reduction in the background signal due to air scattering around the sample as well as minimizing the radiation damage to the films which is observed when annealing in the beam in a nonevacuated environment.

Results and Discussion

We present results of in-situ grazing incidence X-ray diffraction measurements in the GISPS geometry for PET films annealed at a range of temperatures between 85 and 100 °C. These build on previous work,[8] in which we performed GIXRD scans in both GISPS and GIABS geometries on a range of different samples annealed ex-situ at different temperatures for 24 h when crystallization is fully progressed. The two main features of the results were (i) more complete crystallization at the surface than in the bulk at temperatures between 85 and 100 °C and (ii) anisotropy in the scattering between the GISPS and GIABS, indicating that the PET chains crystallize with the benzene rings parallel to the surface. In this study, we extend these measurements to in-situ studies of crystallization in order to probe the kinetics of the crystallization process at the surface and in the bulk of the material.

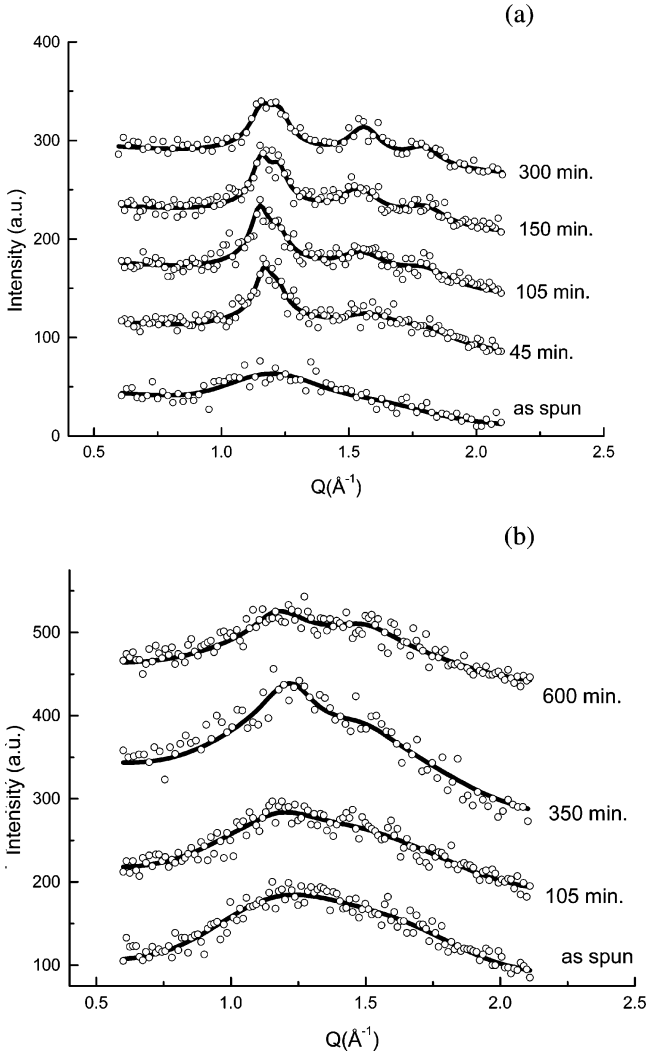

Figure 3. In-situ GISPS scans for (a) the surface ($\alpha = 0.18°$) and (b) bulk ($\alpha = 0.60°$) of a PET film annealed at 95 °C for the times indicated.

Figure 3 shows scans in the GISPS geometry for the surface (taken at an angle of incidence of $\alpha = 0.18°$) and the bulk ($\alpha = 0.60°$) of a PET film annealed at 95 °C for the times indicated. It is clear from these data that there are quite significant differences between the surface and bulk crystallization behavior in the thin film. The spin-cast films before annealing show a broad amorphous hump for all angles of incidence, confirming that no crystalline ordering exists in the as-spun state. In the in-situ surface scans, a clearly defined peak at $Q \approx 1.15$ Å^{-1} is observed within 45 min of the anneal commencing. As annealing continues, in addition to this dominant peak a second peak grows at $Q \approx 1.23$ Å^{-1} and broader peaks develop at $Q \approx 1.54$ Å^{-1} and $Q \approx 1.80$ Å^{-1}. These peaks can all be identified with respect to the crystalline unit cell of bulk PET (shown in Figure 4)[22] as the (0 $\bar{1}$ 1), (0 1 0), (1 $\bar{1}$ 1), and (1 0 0) reflections, confirming that the scattering observed arises from crystalline ordering of the polymer. There is little intensity observed for the (1 $\bar{1}$ 0) peak at 1.64 Å^{-1}. The surface scans contrast starkly with those for the bulk, where the dominant peak at $Q \approx 1.23$ Å^{-1} is barely detectable above the background even after annealing for 10 h. Previous data[8] show that diffraction peaks for the bulk are well developed after annealing for 24 h, confirming that the bulk is slowly ordering at this temperature. It is clearly evident from these scans that

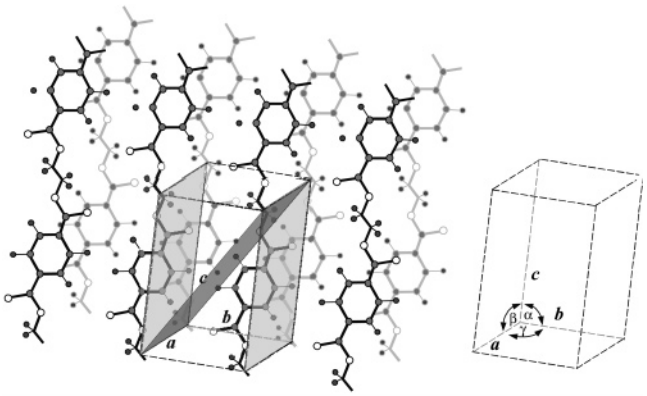

Figure 4. Crystalline unit cell for PET ($a = 4.56$ Å, $b = 5.94$ Å, $c = 10.75$ Å; $\alpha = 98.5°$, $\beta = 118°$, $\gamma = 112°$).[22] The lightly shaded planes denotes the (0 1 0) Miller planes, and the darker shaded plane denotes a (0 $\bar{1}$ 1) plane. The widths of peaks arising from these planes are narrower than for other peaks observed in the GISPS scans as discussed in the text.

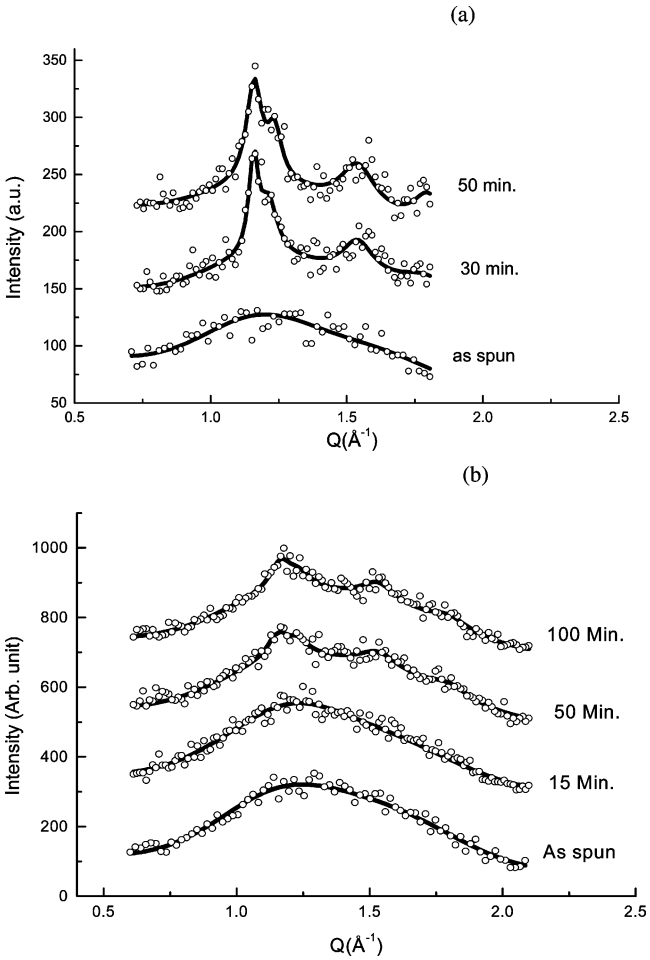

Figure 5. In-situ GISPS scans for (a) the surface ($\alpha = 0.18°$) and (b) bulk ($\alpha = 0.60°$) of a PET film annealed at 100 °C for the times indicated.

the crystallization kinetics are significantly faster at the surface of the thin film. As discussed in the Introduction, there is growing evidence that local segment mobility near the surface of a thin polymer film is enhanced over the bulk, and this is likely to contribute significantly to the faster kinetics observed here.

Figure 5 shows surface and bulk GISPS scans for a PET film annealed in-situ at 100 °C. These data highlight the effect of increasing the annealing temper-

ature on the surface and bulk ordering. The film crystallizes rapidly at the surface, and three well-defined diffraction peaks (with assignments identical to those at 95 °C) are obtained within 30 min of the anneal commencing. In contrast to the 95 °C scans, a high degree of crystalline order is now observed in the bulk on the time scale of the experiment, with the secondary diffraction peaks also detectable. The development of the peaks is slower than at the surface, in agreement with the 95 °C scans. It appears from these results that crystallization, which occurs almost instantly at the surface of the film, propagates into the bulk with further annealing time.[8]

This qualitative description may be quantitatively characterized by least-squares fitting. The measured intensity was fitted with Gaussian and Lorentzian peaks representing the amorphous and crystalline peaks, respectively. Two Gaussian peaks were required to fit the unannealed amorphous film scattering and four Lorentzian peaks to account for the PET crystalline scattering. Fitting the scattering from the unannealed spin-cast scans with just one Gaussian function led to a statistically significant degradation of the fit. We are unclear as to the origin of the double-peak structure in the as-spun samples: it may point to a degree of weak localized ordering induced by the buried interface. The fitted function, representing the summation over these Gaussian and Lorentzian peaks, was

$$I(Q) = B_0 + B_1 Q + A_G \sum_g m_g \left(\frac{2\eta}{\pi W_g^2}\right)^{1/2} \times \exp\left[-\frac{1}{2}\frac{\eta(Q-Q_g)^2}{(W_g/2)^2}\right] + A_L \sum_l m_l \frac{1}{\pi}\frac{W_l/2}{(W_l/2)^2 + (Q-Q_l)^2}$$

where $\eta = 2 \ln 2$, B_0 and B_1 represent a linear sloping background, A_g, W_g and A_l, W_l are the area and full width at half-maximum (fwhm) of the Gaussian and Lorentzian peaks, respectively.

As a result of the limited count time inherent in time-resolved scans and weak surface scattering, the scan statistics do not allow all parameters to be freely fitted. The following fit parameter constraints were employed:

The relative peak areas were assumed to remain constant during annealing. The m_g parameters were fitted to scans at room temperature prior to the anneal, and the m_l parameters were fitted to the last scans in a particular time series during an anneal and then fixed for other fits. The two fitting parameters relating to peak areas were A_G and A_L, which together determine the crystalline fraction $\gamma = A_L/(A_L + A_G)$.

In all scans, it was clear that the widths of the (0 $\bar{1}$ 1) and (0 1 0) Lorentzian peaks were narrower than the peaks at higher Q values. These two peaks were assigned a peak width parameter W_{L1}, and the other peaks were assigned a peak width parameter W_{L2}. Both Gaussian peaks were assumed to have equal fixed W_G, determined from the unannealed film.

During a time series of scans, the fitted parameters were A_G and A_L controlling peak areas, W_{L1} and W_{L2} controlling the Lorentzian peak widths, and the background parameters B_0 and B_1. Constraining the fitted parameters in this way enabled the variation of parameters with annealing time to be traced. Allowing additional parameters to vary in the fit gave a greater arbitrary spread in resulting fitted values but did not yield a statistically significant improvement in the χ^2 value. The one temperature at which the surface and bulk kinetics can be compared numerically is 95 °C. At lower temperatures, the bulk crystallization is too slow whereas the surface kinetics can be quantified. At 100 °C, the surface ordering is too fast to perform full scans: we display two short scans which are not sufficiently wide to fit (Figure 5).

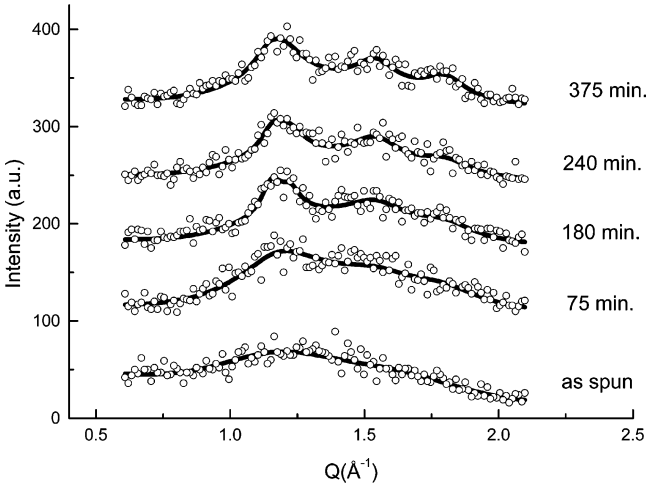

Figure 6. In-situ GISPS scans for the surface of a PET film annealed at 90 °C for the times indicated.

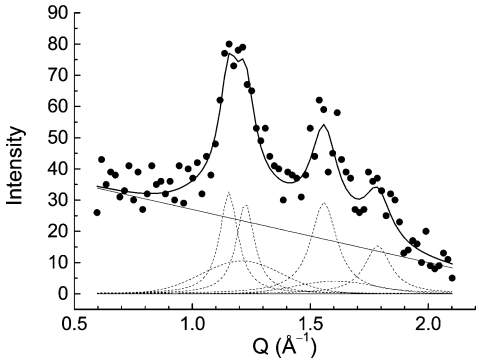

Figure 7. Fits to surface-sensitive GISPS scans using four peaks centered at Q values of 1.15, 1.23, 1.54, and 1.80 Å^{-1} as shown. This example is for a film annealed at 95 °C for 300 min.

The data in Figures 3, 5, and 6 show the fitted curves superimposed onto all the scans. Figure 7 shows the fitted individual Gaussian and Lorentzian peaks for the 95 °C surface-sensitive scan (Figure 3a). The ratio of the total integrated area under Lorentzian peaks to that under the Gaussian peaks is shown in Figure 8a as a function of annealing time. At 95 °C, the fits for the surface and bulk sensitive scans can be compared directly. The Lorentzian:Gaussian area ratio β settles to a value of 3.19 after an annealing time of about 3 h. This ratio corresponds to a crystalline fraction $\gamma = \beta/(1 + \beta) = 0.76 \pm 0.10$. In comparison, the bulk value of β settles to a value of 0.56 corresponding to a value of $\gamma = 0.35 \pm 0.10$. At 90 °C, the bulk crystallization was too slow to measure, and at 100 °C, the surface region crystallized too rapidly to follow. The resulting equilibrium crystalline fractions are summarized in Table 1.

The peak widths provide additional information concerning the crystallization kinetics. The (0 $\bar{1}$ 1) and (0 1 0) surface peaks at 95 °C (Figure 8b) display widths of 0.082 Å^{-1} consistently for the whole time series showing that these peaks are fully developed after an

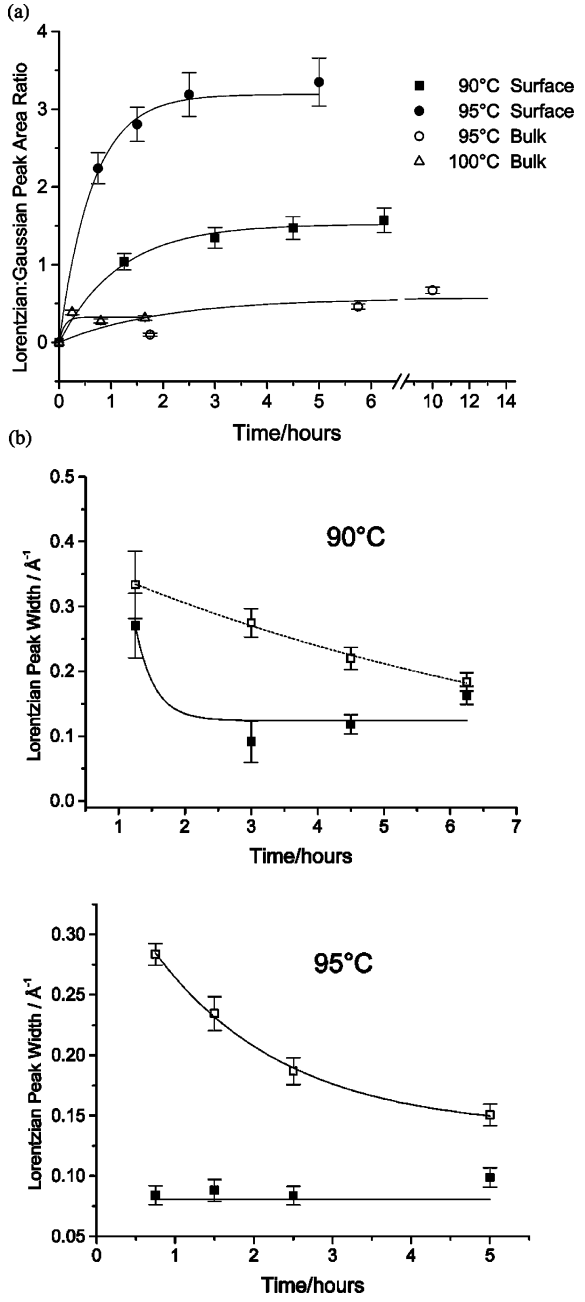

Figure 8. (a) Ratio of Lorentzian to Gaussian peak areas, A_L/A_G, as a function of annealing time at different annealing temperatures. (b) Lorentzian peak widths for (0 1 0) and (0 1 1) peaks (closed symbols) and (1 0 0) and ($\bar{1}$ 1 1) (open symbols) at 90 and 95 °C.

Table 1. Summary of Crystalline Fractions and Domain Sizes

	crystalline fraction	domain size/Å (0,$\bar{1}$,1),(0,1,0)	domain size/Å ($\bar{1}$,1,1),($\bar{1}$,1,0),(1,0,0)
90 °C surface	0.60	46	36
95 °C surface	0.76	67	40
95 °C bulk	0.35	31	18
100 °C bulk	0.25	65	

hour's anneal. The width of the other peaks decreases continuously during the anneal leading to a long-time limit of 0.14 Å^{-1}. The corresponding long-time domain sizes $D = 0.9(2\pi/W_l)$ are 67 Å for the (0 $\bar{1}$ 1) and (0 1 0) peaks and 40 Å for the other peaks. Similar behavior is observed for 90 °C (Figure 8b). This difference in the time variation of the widths indicates that the crystalline domains are extended in the (0 $\bar{1}$ 1) and (0 1 0)

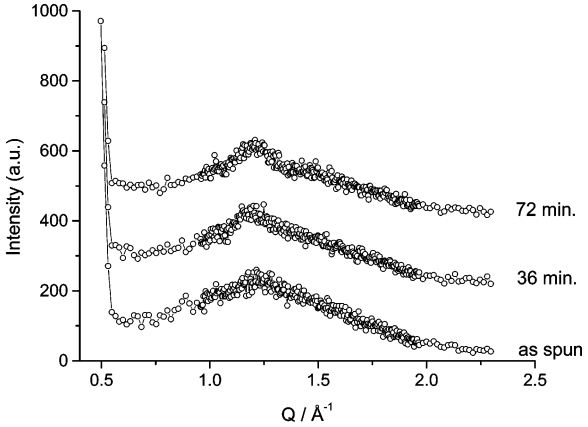

Figure 9. In-situ GISPS scans for the surface of a 180 Å thick PET film annealed at 90 °C for the times indicated. Comparison with the corresponding scan for the 1100 Å thick film in Figure 6 demonstrates that the crystallization rates are similar in both films. It should be noted that the arbitrary intensity scales are different for the two figures, which were performed on separate experiments at ESRF.

reciprocal lattice directions compared to the other directions. Comparison with Figure 4 shows that these reciprocal lattice directions (normal to the corresponding crystal planes) represent directions approximately perpendicular to the chain axis in the plane of the benzene rings. Careful comparison indicates that the samples, spin-cast from trifluoroacetic acid and annealed ex-situ, presented in Figures 2 and 3 of ref 8, exhibit more rapid crystallization in the bulk than those spin-cast from *o*-chlorophenol solution presented here and in Figure 5a of ref 8. It has been reported that TFA can cause transesterification and end group substitution[23,24] in PET, but one would not expect these effects to lead to significantly faster crystallization kinetics in the bulk of the film. Alternatively, it could be suggested that the slower bulk kinetics observed for samples spin-cast from *o*-chlorophenol solution might be caused by suppression of crystallization induced by the buried interface. This can be ruled out by consideration of data for an ultrathin 180 Å thick PET film spin-cast from *o*-chlorophenol solution in Figure 9. The surface crystallization kinetics is not suppressed here by the closeness of the buried interface: crystallization occurs at a similar rate to the thicker films. For all samples, irrespective of surface treatment and the solvent used, crystallization occurs more rapidly at the surface compared with the bulk of the film. However, further work is needed to explore the effect of factors such as surface treatment, solvent effects, and film thickness on the detailed kinetics of crystallization.

Conclusions

In-situ GIXRD has been used to show that, at temperatures just above T_g, crystalline ordering in thin films of PET occurs at a faster rate near to the free surface than in the bulk of the film. Quantitative fits show that the crystalline fraction at the surface is 0.76 at the surface compared with 0.35 in the bulk at 95 °C. The (0 $\bar{1}$ 1) and (0 1 0) peaks narrow more rapidly and achieve a lower width, indicating that the crystallization progresses more rapidly in these crystallographic directions. This enhanced ordering is attributed to a combination of surface energy effects, which promote localized packing, and to an enhanced segmental mobility near the free surface. These results have important implica-

tions for our understanding of the behavior of polymer systems near interfaces.

Acknowledgment. M.D., A.D., and P.C. acknowledge support from EPSRC (GR/M08516), who also funded the XMaS beamline, designed and built by M. Cooper and W. G. Stirling.

References and Notes

(1) van Hutten, P. F.; Krasnikov, V. V.; Hadziioannou, G. In *Conjugated Polymer and Molecular Interfaces*; Salaneck, W. K., Seki, K., Kahn, A., Pireaux, J. J., Eds.; Marcel Dekker: New York, 2001; p 113−152.
(2) Higgins, A. M.; Martin, S. J.; Jukes, P. C.; Geoghegan, M.; Jones, R. A. L.; Langridge, S.; Cubitt, R.; Kirchmeyer, S.; Wehrum, A.; Grizzi, I. *J. Mater. Chem.* **2003**, *13*, 2814−2818.
(3) Higgins, A. M.; Jukes, P. C.; Martin, S. J.; Geoghegan, M.; Jones, R. A. L.; Cubitt, R. *Appl. Phys. Lett.* **2002**, *81*, 4949−4951.
(4) Baschnagel, J.; Binder, K. *Macromolecules* **1995**, *28*, 6808−6818.
(5) Mansfield, K. F.; Theodorou, D. N. *Macromolecules* **1990**, *23*, 4430−4445.
(6) Jones, R. A. L.; Norton, L. J.; Kramer, E. J.; Bates, F. S.; Wiltzius, P. *Phys. Rev. Lett.* **1991**, *66*, 1326−1329.
(7) Geoghegan, M.; Krausch, G. *Prog. Polym. Sci.* **1993**, *28*, 261−302.
(8) Durell, M.; Macdonald, J. E.; Trolley, D.; Wehrum, A.; Jukes, P. C.; Jones, R. A. L.; Walker, C. J.; Brown, S. *Europhys. Lett.* **2002**, *58*, 844−850.
(9) Dalnoki-Veress, K.; Forrest, J. A.; Massa, M. V.; Pratt, A.; Williams, A. *J. Polym. Sci., Part B: Polym. Phys.* **2001**, *39*, 2615−2621.
(10) Forrest, J. A.; Jones, R. A. L. In *Polymer Surfaces, Interfaces and Thin Films*; Karim, A., Kumar, S., Eds.; World Scientific: Singapore, 2000; pp 251−294.
(11) Kawana, S.; Jones, R. A. L. *Phys. Rev. E* **2001**, *63*, 021501.
(12) Yethiraj, A. *J. Chem. Phys.* **1994**, *101*, 2489−2497.
(13) Heeley, E. L.; Maidens, A. V.; Olmsted, P. D.; Bras, W.; Dolbnya, I. P.; Fairclough, J. P. A.; Terrill, N. J.; Ryan, A. J. *Macromolecules* **2003**, *36*, 3656−3665.
(14) Forrest, J. A.; Dalnoki-Veress, K. *Adv. Colloid Interface Sci.* **2001**, *94*, 167−196.
(15) Hayes, N. W.; Beamson, G.; Clark, D. T.; Law, D. S. L.; Raval, R. *Surf. Interface Anal.* **1996**, *24*, 723−728.
(16) Hyun, J.; Aspnes, D. E.; Cuomo, J. J. *Macromolecules* **2001**, *34*, 2395−2397.
(17) Factor, B. J.; Russell, T. P.; Toney, M. F. *Phys. Rev. Lett.* **1991**, *66*, 1181−1184.
(18) Factor, B. J.; Russell, T. P.; Toney, M. F. *Macromolecules* **1993**, *26*, 2847−2859.
(19) Kawana, S.; Durell, M.; Lu, J.; Macdonald, J. E.; Grell, M.; Bradley, D. D. C.; Jukes, P. C.; Jones, R. A. L.; Bennett, S. L. *Polymer* **2002**, *43*, 1907−1913.
(20) Macdonald, J. E.; Durell, M.; Trolley, D.; Lei, C.; Das, A.; Jukes, P. C.; Geoghegan, M.; Higgins, A. M.; Jones, R. A. L. *Radiat. Phys. Chem.* **2004**, *71*, 811−815.
(21) Sirringhaus, H.; Brown, P. J.; Friend, R. H.; Nielsen, M. M.; Bechgaard, K.; Langeveld-Voss, B. M. W.; Spiering, A. J. H.; Janssen, R. A. J.; Meijer, E. W.; Herwig, P.; de Leeuw, D. M. *Nature (London)* **1999**, *401*, 685−688.
(22) De Daubeny, R. P.; Bunn, C. W.; Brown, C. J. *Proc. R. Soc. London* **1954**, *A226*, 531−542.
(23) Kenwright, A. M.; Peace, S. K.; Richards, R. W.; Bunn, A.; MacDonald, W. A. *Polymer* **1999**, *40*, 5851−5856.
(24) Collins, S.; Kenwright, A. M.; Pawson, C.; Peace, S. K.; Richards, R. W.; MacDonald, W. A.; Mills, P. *Macromolecules* **2000**, *33*, 2974−2980.

MA0490606